*Thermochimica Acta*, 58 (1982) 45-51
Elsevier Scientific Publishing Company, Amsterdam – Printed in The Netherlands



# A THERMOGRAVIMETRIC AND ELECTRON MICROSCOPY STUDY OF THE DECOMPOSITION OF AKAGANEITE

J.M. GONZALEZ-CALBET

*Departamento de Química Inorgánica, Facultad de Ciencias Químicas, Universidad Complutense, Madrid-3 (Spain)*

M.A. ALARIO FRANCO

*Instituto de Química Inorgánica "Elhuyar", Consejo Superior de Investigaciones Científicas, Madrid-6 (Spain)*

(Received 10 March 1982)

## ABSTRACT

The ferromagnetic oxide $\gamma$-$Fe_2O_3$ is formed by the vacuum thermal decomposition of anhydrous $\beta$-iron oxyhydroxide. In the initial stage the process appears to follow a nucleation and growth mechanism which leads to the formation of a single macropore in every crystal.

## INTRODUCTION

$\beta$-Iron oxyhydroxide (akaganeite) crystallizes in the hollandite structure [1] characterized by the presence of tunnels occupied by water molecules and some chloride ions. Consequently, the elimination of water leads to the formation of an interesting porous system of homogeneous pores [2]. On the other hand, it is well known that $\beta$-FeOOH decomposes to $\alpha$-$Fe_2O_3$ (hematite) on heating [3]. In his early work on electron diffraction of synthetic akageneite, Mackay [4] suggested that $\gamma$-$Fe_2O_3$ (maghemite) was an intermediate stage in the decomposition of $\beta$-FeOOH to $\alpha$-$Fe_2O_3$, and considered a simple mechanism involving migration of iron atoms to explain the topotactic dehydration of $\beta$-iron oxyhydroxide to $\gamma$-$Fe_2O_3$. Since the heating of anhydrous $\beta$-FeOOH leads to the formation of a new porous system [5], a more detailed study of the different stages of decomposition of synthetic akaganeite was considered worthwhile. In this paper, we present a study of the thermal decomposition of $\beta$-FeOOH under vacuum by means of thermogravimetry and electron microscopy.

0040-6031/82/0000-0000/$02.75 

TABLE 1

Products of the thermal decomposition.

| $T$(°C) | Products |
|---|---|
| 200, 221, 246 | $\beta$-FeOOH |
| 271, 298, 310, 320 | $\beta$-FeOOH and $\gamma$-$Fe_2O_3$ |
| 340 | $\gamma$-$Fe_2O_3$ and $\alpha$-$Fe_2O_3$ |
| 367 | $\alpha$-$Fe_2O_3$ |

## EXPERIMENTAL

Anhydrous $\beta$-FeOOH was prepared [6] by heating $\beta$-FeOOH $\cdot$ $n$ $H_2O$ under vacuum at 150°C. $\beta$-FeOOH $\cdot$ $n$ $H_2O$ was synthesized by hydrolizing a $FeCl_3 \cdot 6$ $H_2O$ solution (2% in weight) at 60°C for 24 h. The chloride content of the $\beta$-FeOOH was estimated to be 2% [5,6]. Thermal decomposition experiments were carried out on a Cahn microbalance fitted to a vacuum line ($P < 10^{-4}$ torr) in the temperature range 200–370°C. The final products of the thermal decomposition, as characterized by both X-ray and electron diffraction, are shown in Table 1. Electron microscopy was performed on a Siemens Elmiskop 102.

## RESULTS AND DISCUSSION

In order to elucidate the mechanism of the decomposition, we have plotted the extent of decomposition $\alpha$ vs. the reduced time $t/t_{0.5}$ at several temperatures (Fig. 1). In the region $0 < t/t_{0.5} \leq 1$ the values of $\alpha$ appear to follow the Avrami–Erofe'ev equation [7] [eqn. (1)] while in the $1 < t/t_{0.5} \leq 3$ region, they seem to correspond to the Ginstling–Brounshtein–Valensi equation [8,9] [eqn. (2)]

$$[-\ln(1-\alpha)]^{1/3} = Kt \tag{1}$$

$$\left[1-(1-\alpha)^{1/3}\right]^2 = Kt \tag{2}$$

Plots of $[-\ln(1-\alpha)^{1/3}]$ and $[1-(1-\alpha)^{1/3}]^2$ as a function of time for various temperatures are shown in Figs. 2 and 3. The experimental data fall on a straight line for $\alpha$ values between 0 and 0.5 in the case of the first equation and between 0.5 and 0.7 for the second.

If the Avrami–Erofe'ev model were correct one could explain the early part of the thermal decomposition of $\beta$-FeOOH as an instantaneous nuclea-

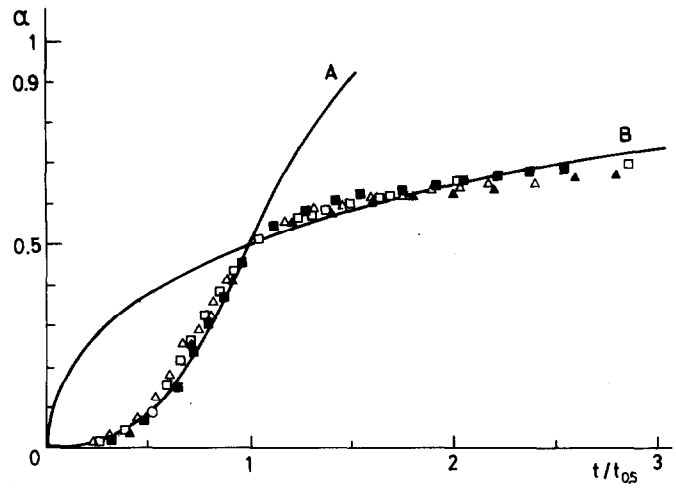


Fig. 1. Reduced time plot in the thermal decomposition of synthetic β-FeOOH under vacuum at several temperatures. Curve A: eqn. (1), Avrami–Erofe'ev; Curve B: eqn. (2), Ginstling–Brounshtein–Valensi. □, 297°C; △, 310°C; ■, 320°C; ▲, 340°C.

tion followed by growth. From the linear transform of eqn. (1) (Fig. 2) and an Arrhenius type plot (Fig. 4) one obtains an activation energy of ~ 7.5 kcal $mole^{-1}$ for $\alpha$ values between 0 and 0.5. There is a problem, however, in that in vacuum thermal decompositions, heat conduction is quite poor and there

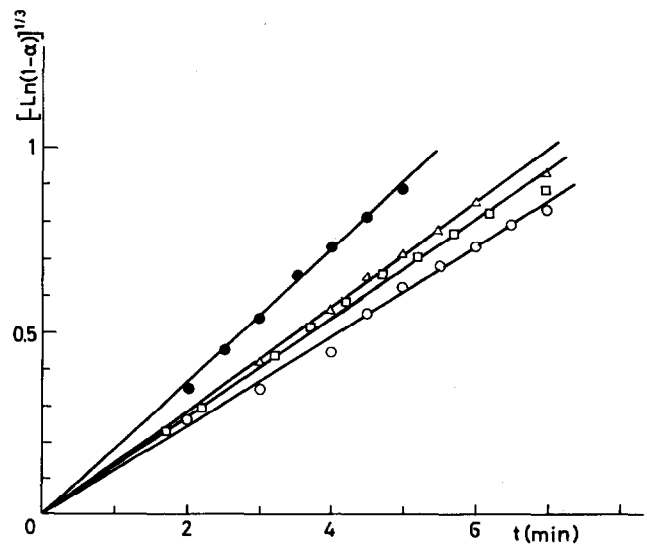


Fig. 2. Reduction isotherms according to the Avrami–Erofe'ev equation. ○, 297°C; □, 310°C; △, 320°C; ●, 340°C.

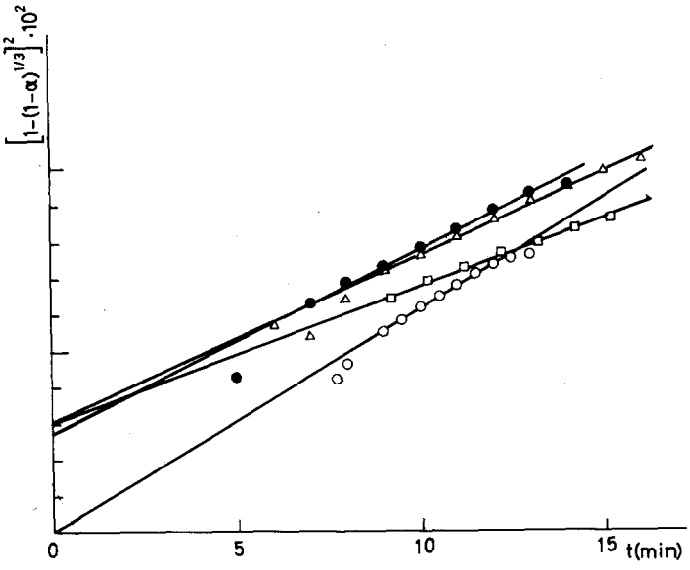


Fig. 3. Reduction isotherms according to the Ginstling–Brounshtein–Valensi equation. ○, 297°C; □, 310°C; △, 320°C; ●, 340°C.

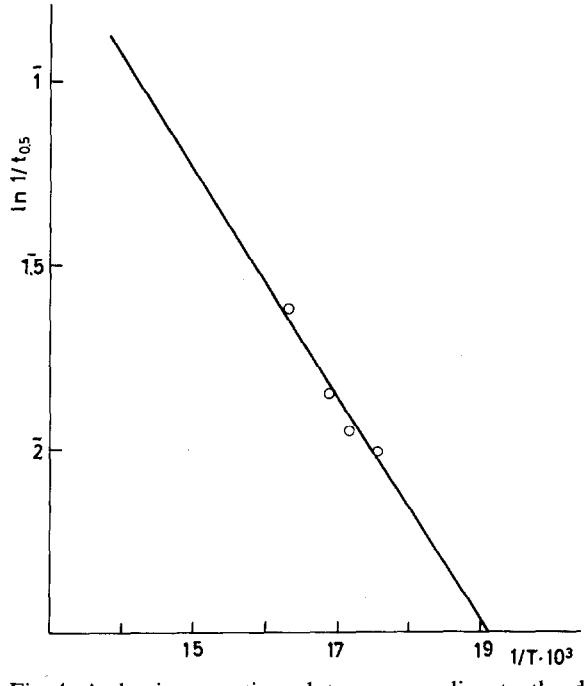


Fig. 4. Arrhenius equation plot corresponding to the decomposition of akaganeite to maghemite ($0 < \alpha \leq 0.5$).

is considerable time lag before the sample attains the decomposition temperature; so the above results are not under strictly isothermal conditions.

With regards to the second step, the fact that the three-dimensional diffusion controlled equation is followed seems to imply that the amount of product formed retards, to some extent, the elimination of the remaining water according to the process.

$$2\ \beta\text{-FeOOH} \rightarrow \gamma\text{-}Fe_2O_3 + H_2O \qquad (3)$$

However, as the range of $\alpha$ values for which the Ginstling–Brounshtein–Valensi equation is followed is quite narrow, $0.5 \leqslant \alpha \leqslant 0.7$, not much significance should be attributed to the activation energy in this region. High-resolution electron microscopy work, nevertheless, shows that this picture is close to reality. Figure 5(a) shows an electron micrograph of $\beta$-FeOOH heated up to $\alpha = 0.3$ (i.e., within the Avrami–Erofe'ev equation range). The numerous holes in the crystal are presumably the growing nuclei which have a large enough size to be observed at the operating wave length. Figure 5(b), on the other hand, shows the same sample at a further stage of decomposition in which overlapping and coalescence of the growing nuclei have produced a macropore in most crystals, as seen in detail in Fig. 5(c). At this stage the sample has more than 50% $\gamma$-$Fe_2O_3$ and this, being much more compact than the original hollandite-type material, can retard the elimination of further OH groups [c.f. eqn. (3)].

For $\alpha$ values over 0.7 the experimental data do not fit any of the usual models for the thermal decomposition of solids. This seems to indicate that the final stages of the decomposition must have a more complex mechanism. The mechanism suggested by Mackay [4] required only the migration of some iron from octahedral to tetrahedral voids and a slight expansion of the $d_{O-O}$ distance (from 3.49 to 4.17 Å) in one direction and a contraction (from 3.49 to 2.95 Å) in another direction. The formation of macropores as shown by our high-resolution electron microscopy work suggests, however, that there is considerable diffusion of both iron and oxygen during the decomposition.

It is interesting to note that Ishikawa and Inouye [10] obtained activation energies of 6.9, 28.6 and 38.18 kcal $mole^{-1}$ for three processes observed, at 70, 180 and 260°C, in their TPD measurements. They attributed the first process to the elimination of water from the hollandite structure, which, obviously, requires a small activation energy and the two other processes to the elimination of surface and bulk OH groups, respectively. Our results, however, show that nucleation of the $\gamma$-$Fe_2O_3$ phase starts, ~ 180°C, at both the surface and the bulk of the crystal and, consequently, it is difficult to distinguish between the two kinds of OH groups. The peaks at 180°C and 260°C as observed by Ishikawa and Inouye in their TPD measurements may

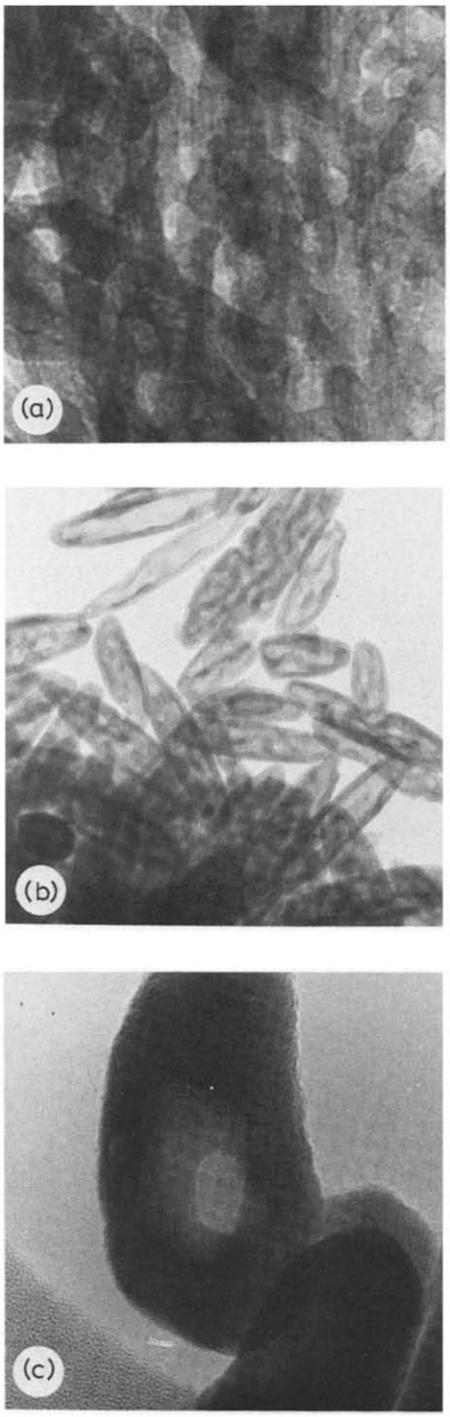


Fig. 5. (a) HREM of $\beta$-FeOOH decomposed in vacuum at 320°C for 5 min ($\alpha = 0.3$). Magnification $1.3 \times 10^6$. (b) HREM of $\beta$-FeOOH decomposed in vacuum at 320°C for 1 h ($\alpha = 0.85$). Magnification $4.5 \times 10^5$. (c) HREM of $\beta$-FeOOH decomposed in vacuum for 1 h. A single pore is present in each crystal. Magnification $1.1 \times 10^6$.

be due to a change in mechanism (at $\alpha \simeq 0.7$) and the consequent change in the activation energy.

## CONCLUSIONS

The present study of the thermal decomposition of synthetic akaganeite confirms the analysis of the evolution of the porous texture as measured by nitrogen adsorption [5]. Although an examination of the hollandite and spinel structures might lead one to believe that decomposition of $\beta$-FeOOH to $\gamma$-$Fe_2O_3$ occurs via the migration of iron along tetrahedral voids with only a slight movement of the oxygen atoms, our results clearly show the necessity of considering diffusion of both iron and oxygen atoms.

## REFERENCES

1 A.L. Mackay, Mineral. Mag., 32 (1960) 545.
2 J.M. González-Calbet and M. Alario-Franco, An. Quím., 77 (1981) 19.
3 R.C. Mackenzie, Differential Thermal Analysis. Vol. 1, Academic Press, London, 1970.
4 A.L. Mackay, Reactivity of Solids Vol. 4, Elsevier, Amsterdam 1961, p. 571.
5 J.M. González-Calbet, M.A. Alario-Franco and M. Gayoso, J. Inorg. Nucl. Chem., 43 (1981) 257.
6 J.M. González-Calbet, Thesis, Universidad Complutense, Madrid, 1979.
7 A.M. Avrami, J. Chem. Phys., 9 (2) (1941) 177. B.U. Erofe'ev, C. R. (Dokl.) Acad. Sci. U.R.S.S., 52 (1946) 511.
8 A.M. Ginstling and B.I. Brounshtein, J. Appl. Chem. U.S.S.R., 23 (1950) 1327.
9 G. Valensi, J. Chem. Phys., 47 (1950) 489.
10 T. Ishikawa and K. Inouye, J. Therm. Anal., 10 (1976) 399.